

DEPARTMENT OF CIVIL ENGINEERING
SCHOOL OF ENGINEERING
OLD DOMINION UNIVERSITY
NORFOLK, VIRGINIA 23508

DATA/LANGLEY
IN-39
64769-CR
P.28

TWO-DIMENSIONAL FINITE ELEMENT ANALYSIS
OF RECTANGULAR PANEL WITH HOLE USING NICE/SPAR

OS 853217
JW

By

Zia Razzaq, Principal Investigator,

Venkatesh Prasad, Graduate Student,

and

Siva Prasad Darbhamulla, Graduate Student

Progress Report

For the period ended December 31, 1986

Prepared for the
National Aeronautics and Space Administration
Langley Research Center
Hampton, Virginia 23665

Under

Research Grant NAG-1-438

Dr. Olaf O. Storaasli, and

Dr. W. Jefferson Stroud, Technical Monitors

SSD-Structural Mechanics Branch

(NASA-CR-180630) TWO-DIMENSIONAL FINITE
ELEMENT ANALYSIS OF RECTANGULAR PANEL WITH
HOLE USING NICE/SPAR Progress Report, period
ended 31 Dec. 1986 (Old Dominion Univ.) 28
p Avail: NTIS HC A03/HF A01 CSCL 20K G3/39

N87-27217

Unclas
0064769

April 1987

DEPARTMENT OF CIVIL ENGINEERING
SCHOOL OF ENGINEERING
OLD DOMINION UNIVERSITY
NORFOLK, VIRGINIA 23508

TWO-DIMENSIONAL FINITE ELEMENT ANALYSIS
OF RECTANGULAR PANEL WITH HOLE USING NICE/SPAR

By

Zia Razzaq, Principal Investigator,

Venkatesh Prasad, Graduate Student,

and

Siva Prasad Darbhamulla, Graduate Student

Progress Report

For the period ended December 31, 1986

Prepared for the
National Aeronautics and Space Administration
Langley Research Center
Hampton, Virginia 23665

Under

Research Grant NAG-1-438

Dr. Olaf O. Storaasli, and

Dr. W. Jefferson Stroud, Technical Monitors
SSD-Structural Mechanics Branch

Submitted by the

Old Dominion University Research Foundation

P.O. Box 6369

Norfolk, Virginia 23508



April 1987

C. Isotropic Panel

The following material properties are adopted for the isotropic panel:

$$E = 10,000 \text{ ksi}$$

$$\nu = 0.3$$

which correspond to those of a typical aluminum alloy. Tables 1 and 2 present a summary of the results for the quadrilateral, and triangular isotropic elements. In these tables, the number of elements used for one-fourth of the panel, the total CPU time for each computer run, the largest principal compressive stress, σ_{\max} , and the corresponding element number are given. Figure 16 gives the graphical representation of the relationships between σ_{\max} and the number of finite elements used. Clearly, the triangular elements provide a better estimate of the maximum stress (whose theoretical limiting value is 3.0). Figure 17 shows the relationships between CPU time and the number of finite elements. The difference between the CPU time with 120 quadrilateral elements and 240 triangular elements is not dramatic. The information in Figures 16 and 17 leads to the conclusion that the triangular elements are more suitable than the quadrilateral ones, for the two-dimensional stress analysis problem considered here.

D. Orthotropic Panel

The following material properties are adopted for the orthotropic panel:

$$E_x = 10,000 \text{ ksi}$$

$$E_y = 1,000 \text{ ksi}$$

$$\nu = 0.3$$

Tables 3 and 4 present a summary of the results for the quadrilateral and

triangular orthotropic elements. Figures 18, and 19 are the corresponding σ_{\max} , and CPU time versus the number of finite elements used, respectively. In this study, it is assumed that the NICE/SPAR program automatically accounts for the necessary transformations of material properties and stresses from the global to local coordinates and vice versa. Thus, the validity of the results for the orthotropic panel depends on the correctness or otherwise of this assumption. Figure 18 shows a significant difference between the σ_{\max} values for the quadrilateral and triangular discretizations. Figure 19 exhibits the same general character for the orthotropic panel as seen earlier in Figure 17 for the isotropic panel. Figure 20 shows how the value of σ_{\max} is affected due to a variation in the E_y/E_x ratio when 160 triangular elements are used. For $E_y/E_x = 1.0$, the σ_{\max} value from the plot agrees with that obtained earlier using the isotropic triangular discretization. For other E_y/E_x values in the range from 0.1 to 1.0, a smooth curve follows. However, the validity of this curve also depends on whether or not NICE/SPAR is handling the necessary transformations properly.

E. On-Going Study

A three-dimensional stress analysis near the hole as well as the use of substructuring and subsequent parallelization of computations are included in the present research activity.

F. Publication

A paper titled "Concurrent Processing for Nonlinear Analysis of Hollow Rectangular Structural Sections," by Siva P. Darbhamulla, Zia Razzaq, and Olaf O. Storaasli, has been accepted for publication in Engineering with Computers: An International Journal for Computer-aided Mechanical and Structural Engineering, 1987.

Table 1. Summary of results for rectangular panel with hole
using E41 (NICE/SPAR) quadrilateral isotropic elements

Number of elements	C P U Time (secs)	Element No. with σ_{max}	σ_{max} (ksi)
12	65.5	4	1.35
22	73.9	7	1.97
36	88.1	7	1.98
48	104.2	11	2.03
68	126.7	11	2.03
80	146.3	22	2.11
120	248.4	61	2.13

Table 2. Summary of results for rectangular panel with hole using E31 (NICE/SPAR) triangular isotropic elements

Number of elements	C P U Time (secs)	Element No with σ_{max}	σ_{max} (ksi)
24	69.9	8	1.76
44	80.8	11	2.38
72	96.1	11	2.39
96	120.2	15	2.49
136	142.9	15	2.50
160	164.1	29	2.67
240	285.7	71	2.74

Table 3. Summary of results for rectangular panel with hole using E41 (NICE/SPAR) quadrilateral orthotropic elements

Number of elements	C P U Time (secs)	Element No. with σ_{max}	σ_{max} (ksi)
12	68.6	5	1.47
22	78.4	7	1.60
36	88.7	7	1.62
48	105.5	13	1.64
68	127.1	13	1.61
80	146.7	25	1.66
120	243.7	72	1.95

NOTE: $E_x = 10,000$ ksi ; $E_y = 1,000$ ksi.

Table 4. Summary of results for rectangular panel with hole
using E31 (NICE/SPAR) triangular orthotropic elements

Number of elements	C P U Time (secs)	Element No. with σ_{max}	σ_{max} (ksi)
24	72.8	16	3.78
44	87.8	22	3.84
72	107.8	22	3.91
96	123.9	42	4.54
136	160.6	42	5.14
160	174.7	72	5.24
240	308.6	176	4.94

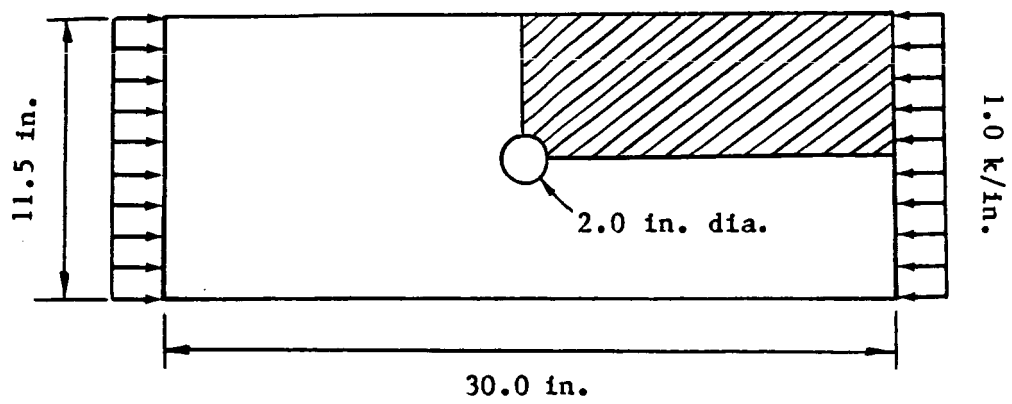


Figure 1. Panel geometry and loading

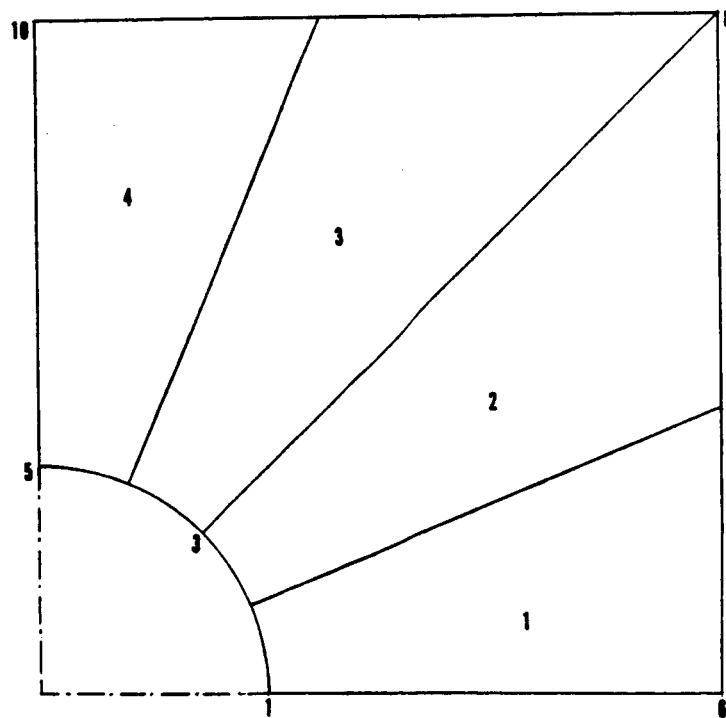
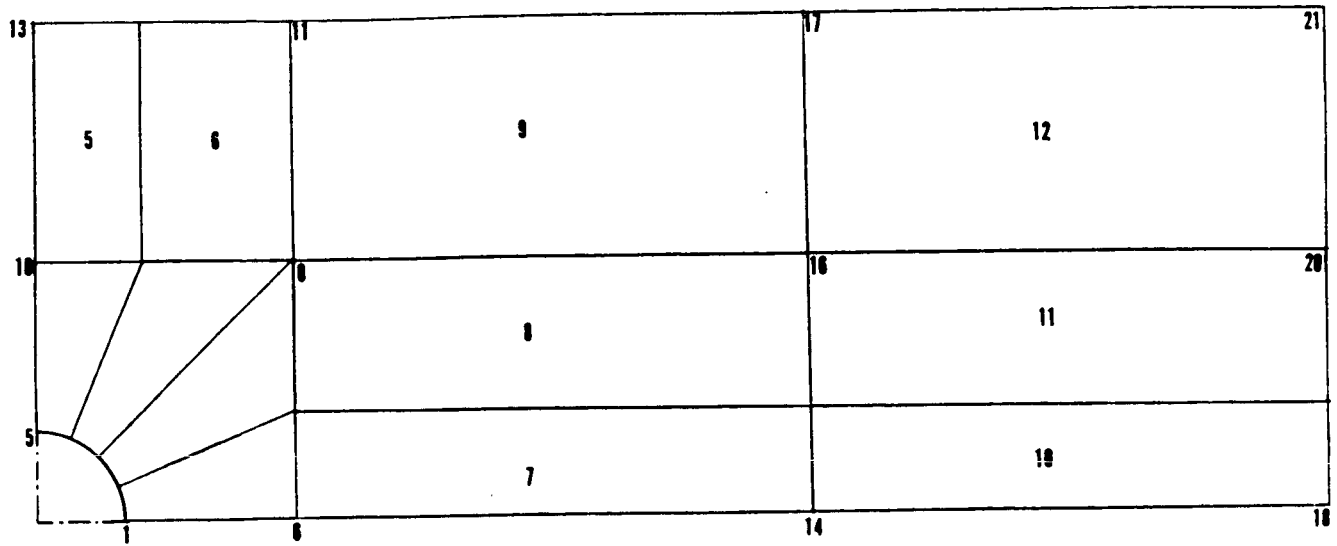


Figure 2. Discretization with 12 quadrilateral elements

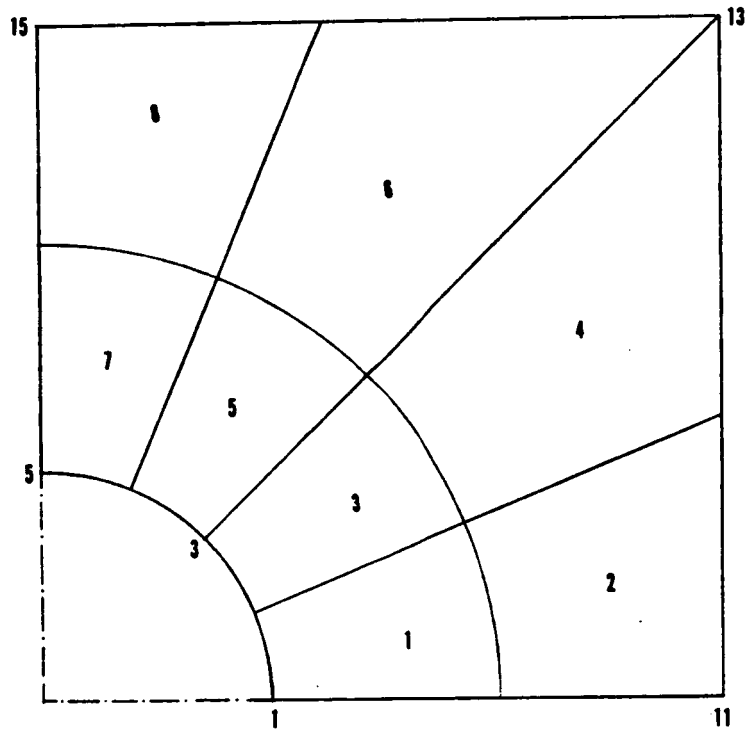
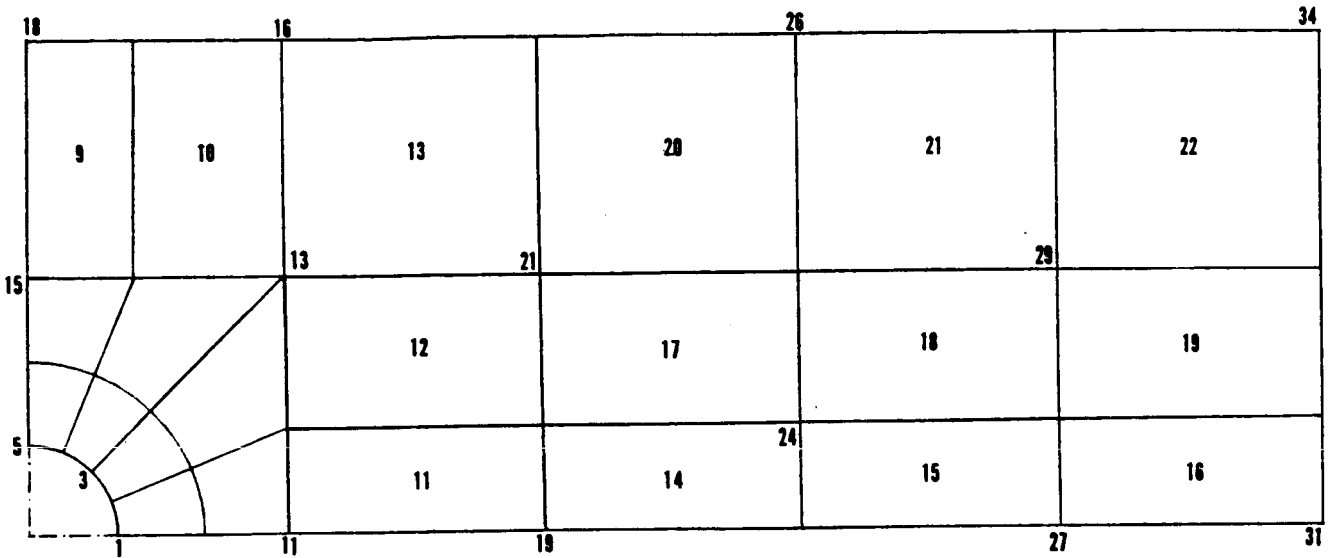


Figure 3. Discretization with 22 quadrilateral elements

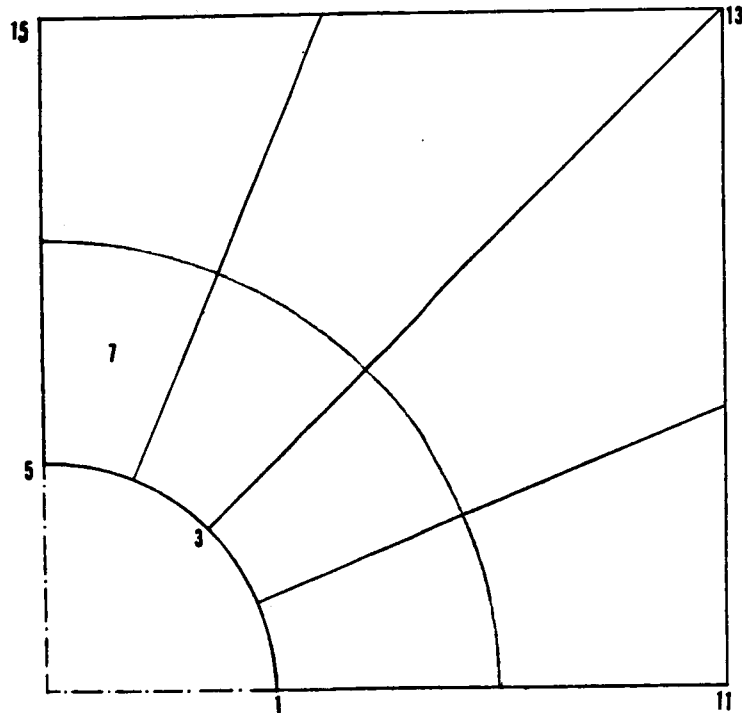
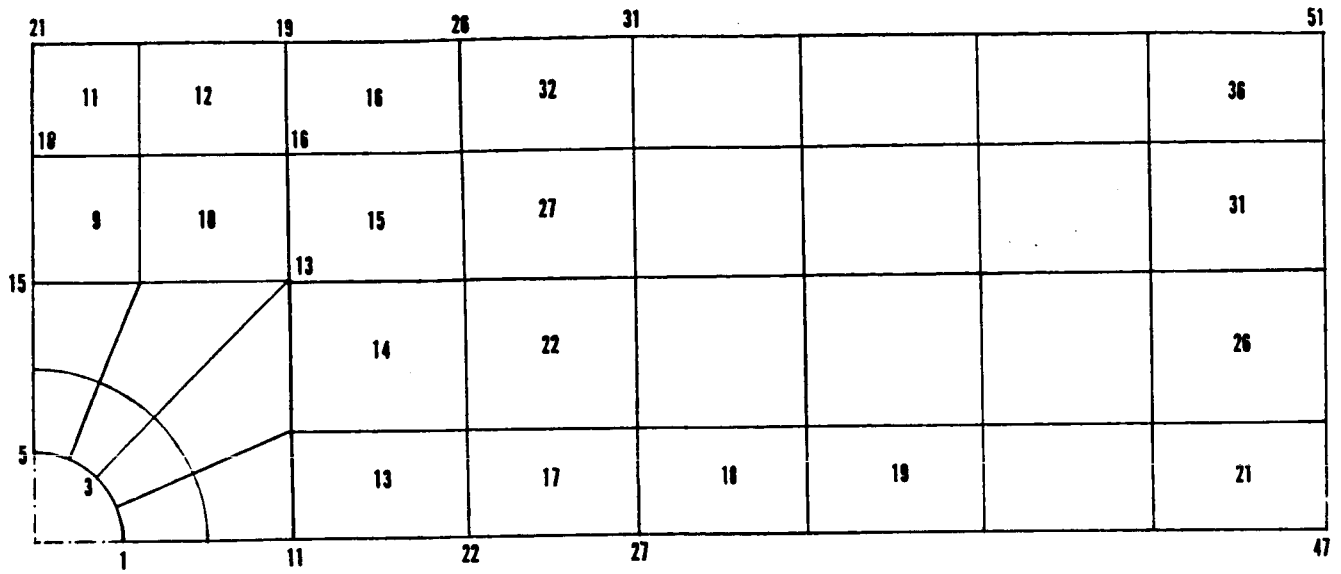


Figure 4. Discretization with 36 quadrilateral elements

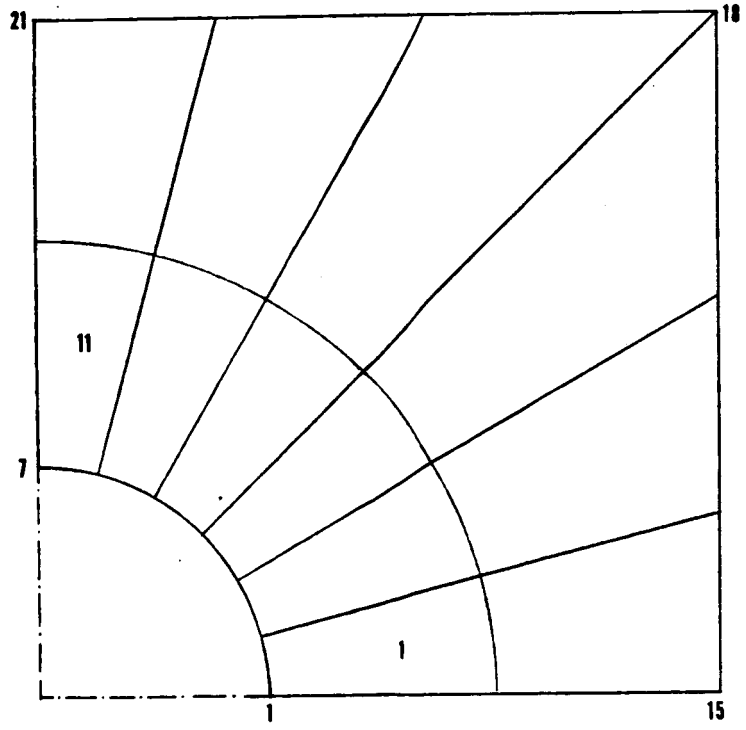
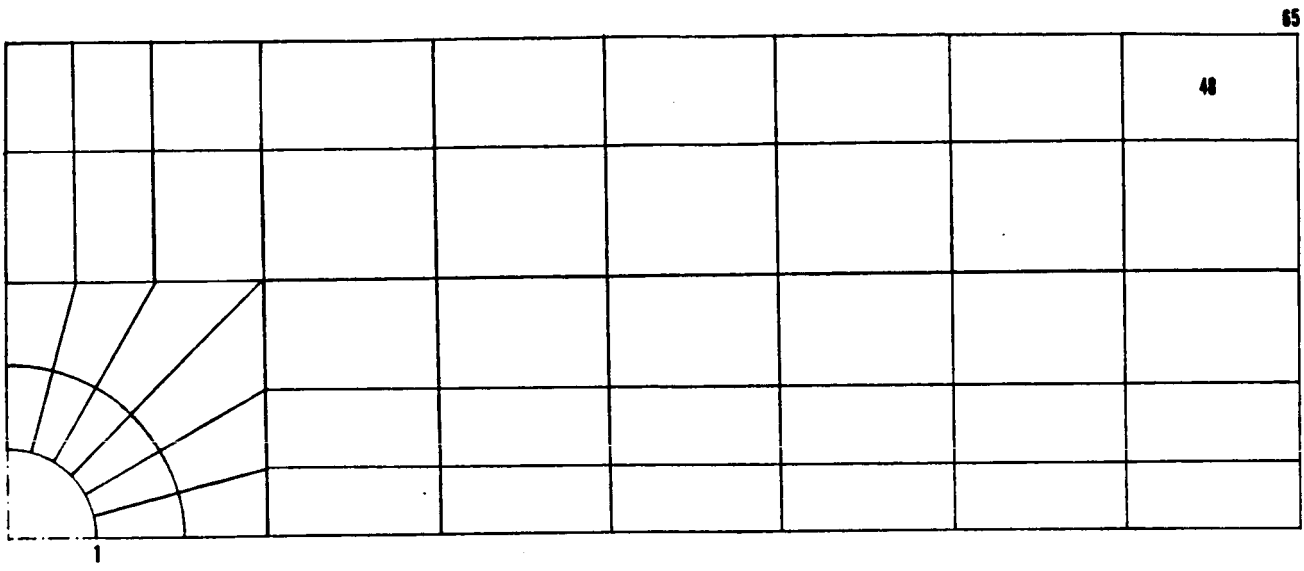


Figure 5. Discretization with 48 quadrilateral elements

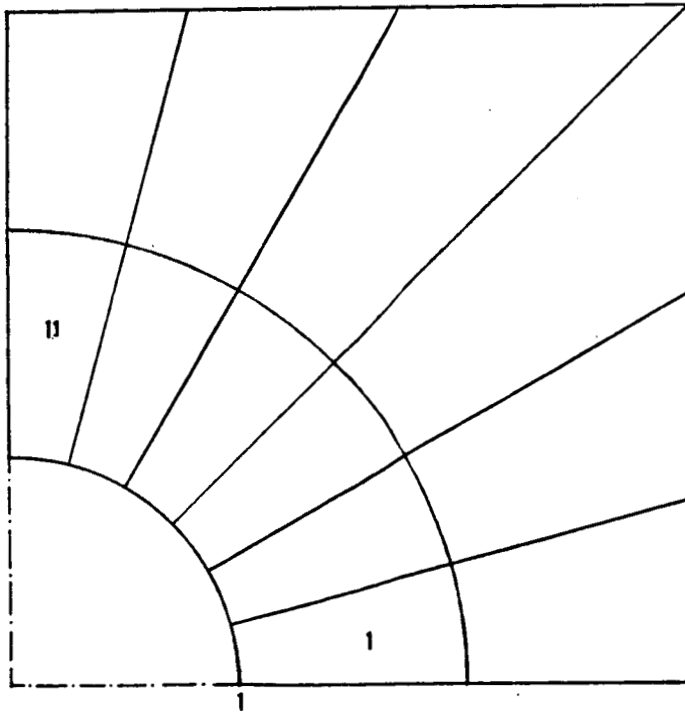
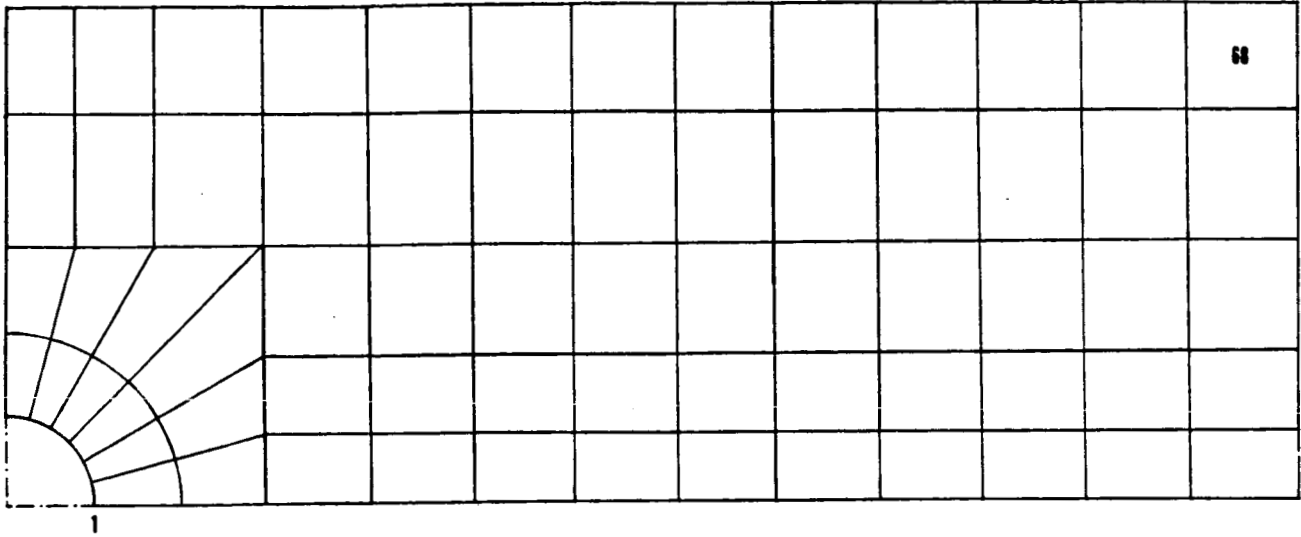


Figure 6. Discretization with 68 quadrilateral elements

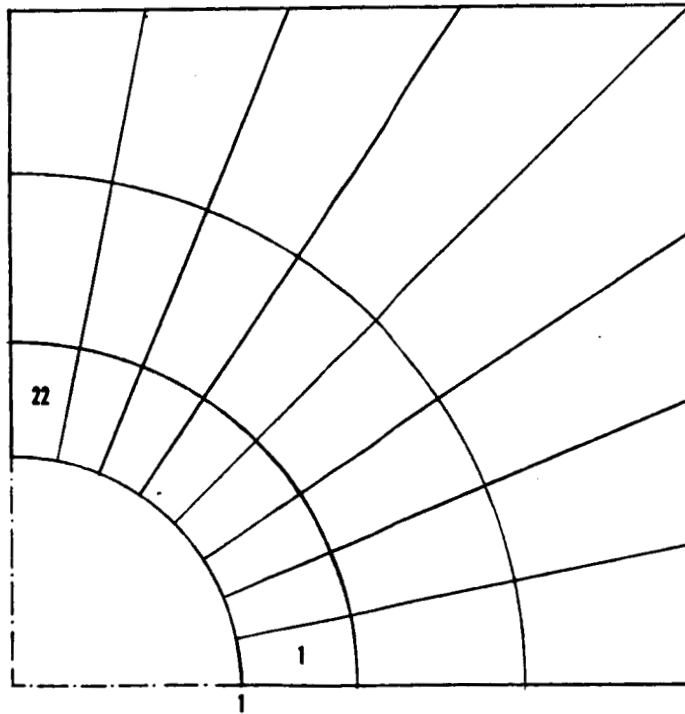
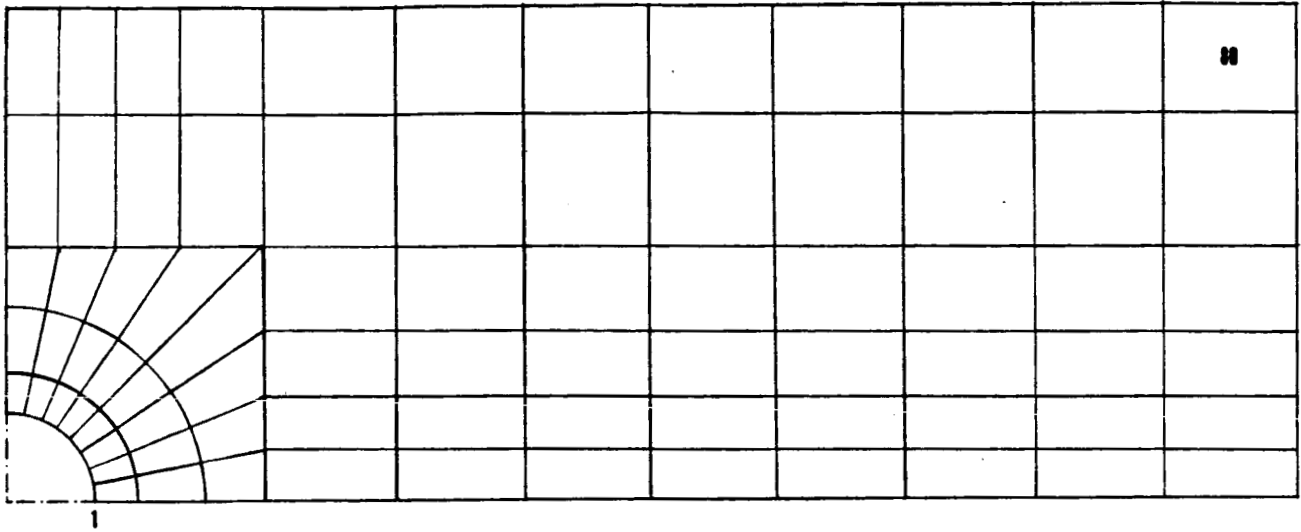


Figure 7. Discretization with 80 quadrilateral elements

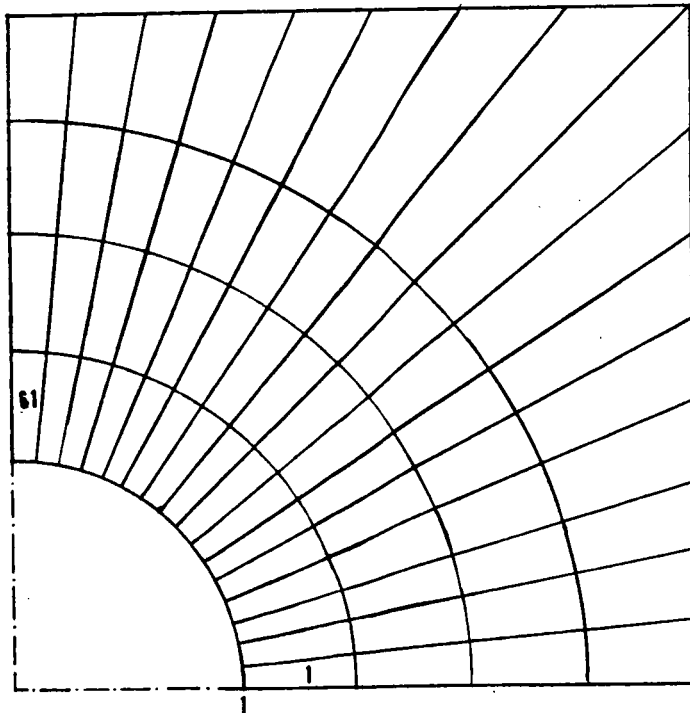
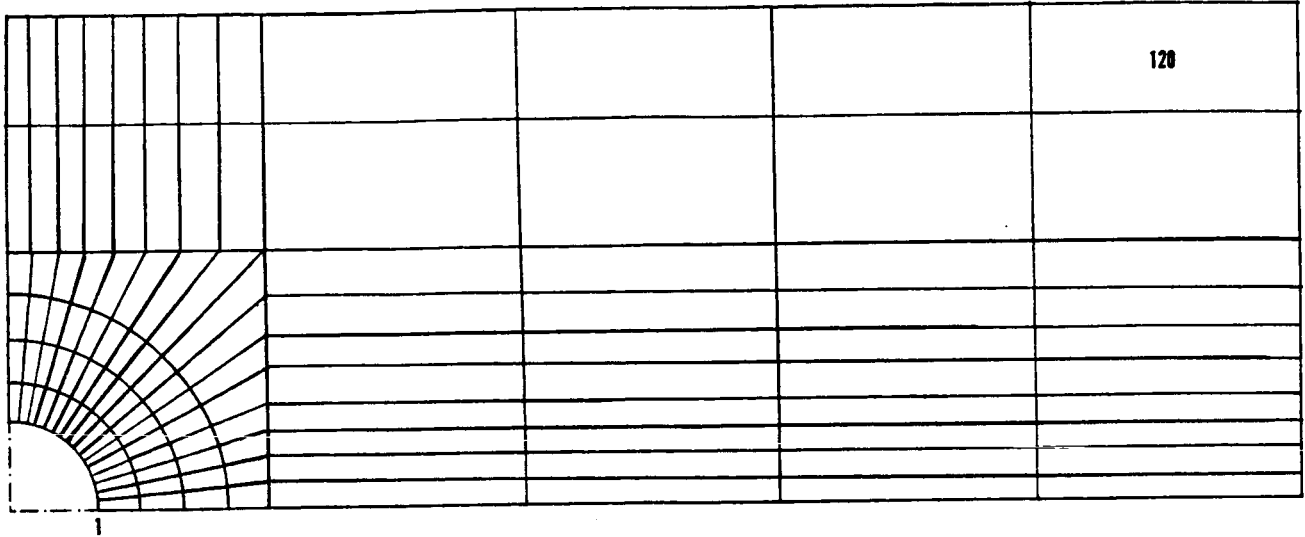


Figure 8. Discretization with 120 quadrilateral elements

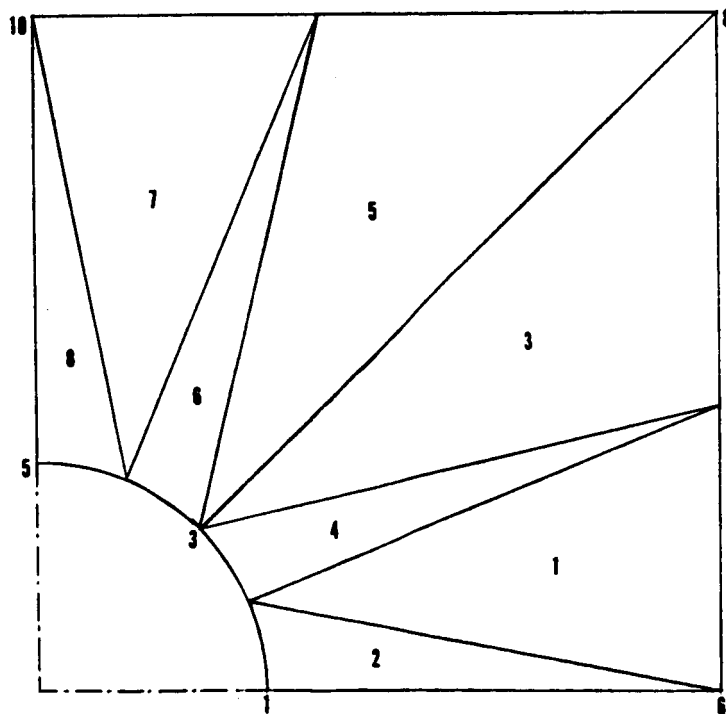
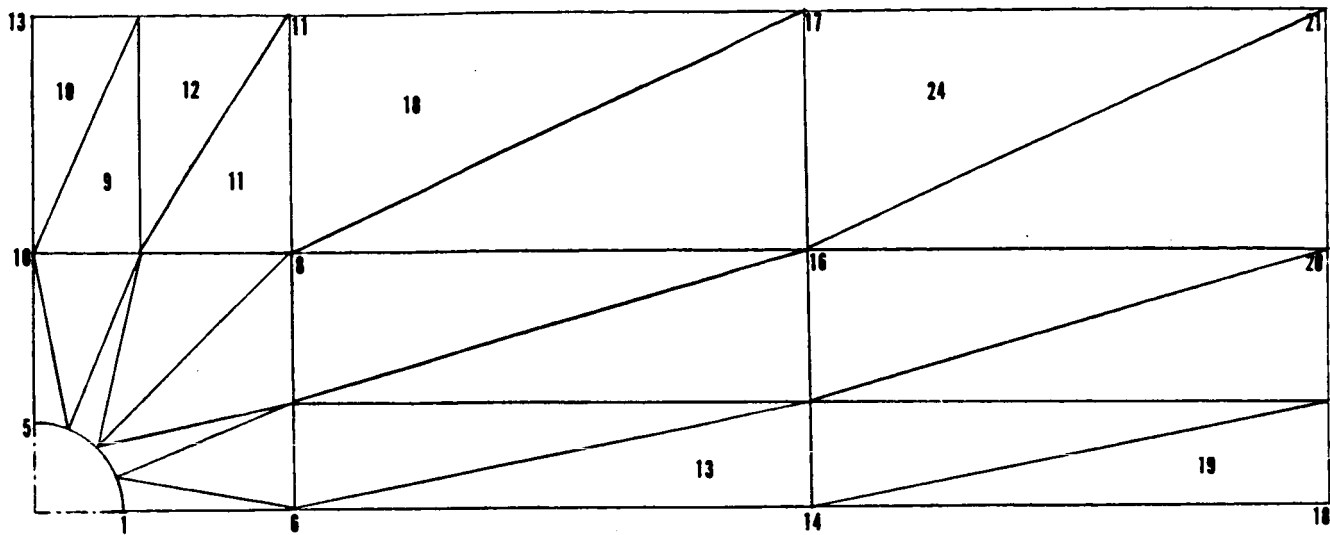


Figure 9. Discretization with 24 triangular elements

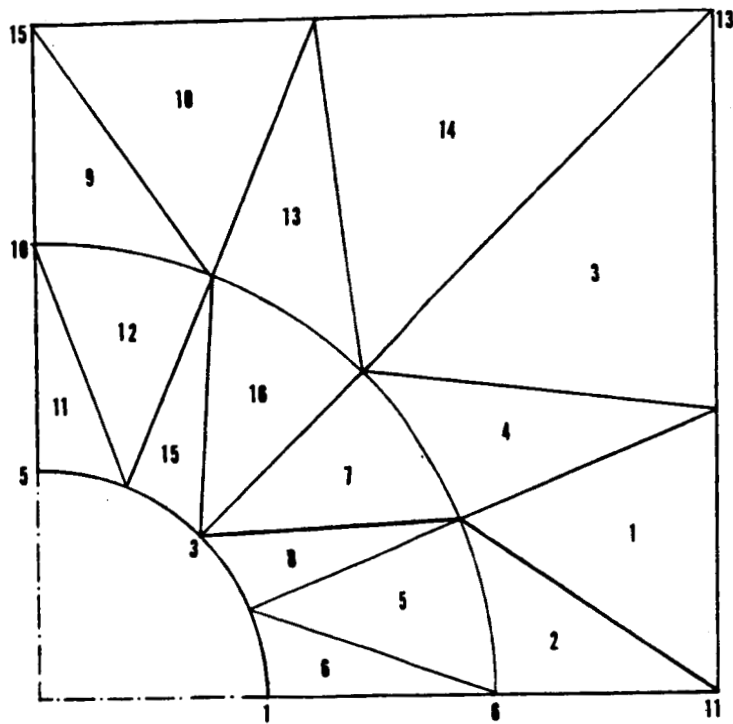
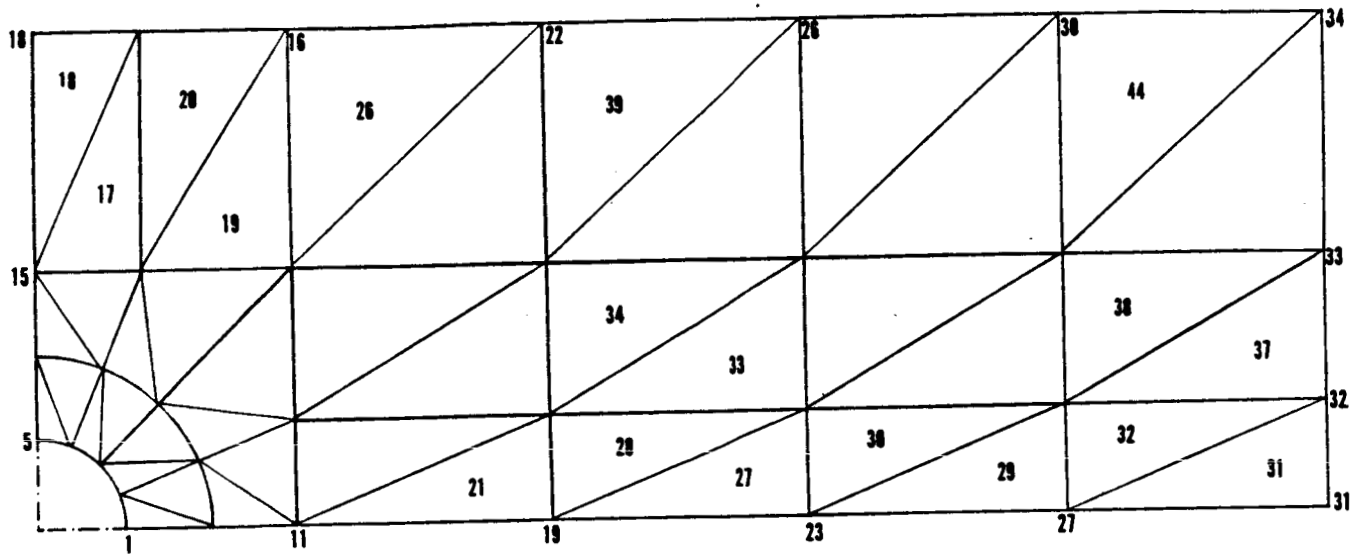


Figure 10. Discretization with 44 triangular elements

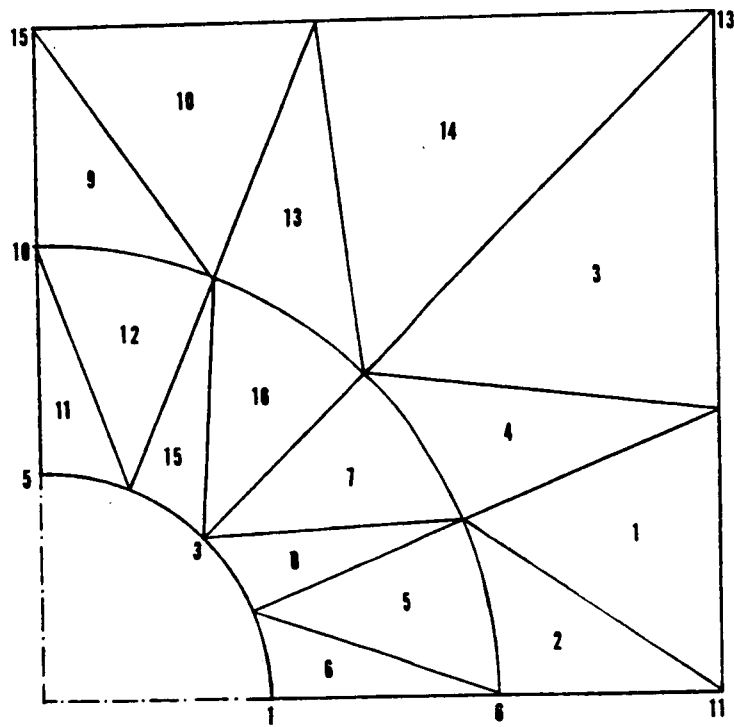
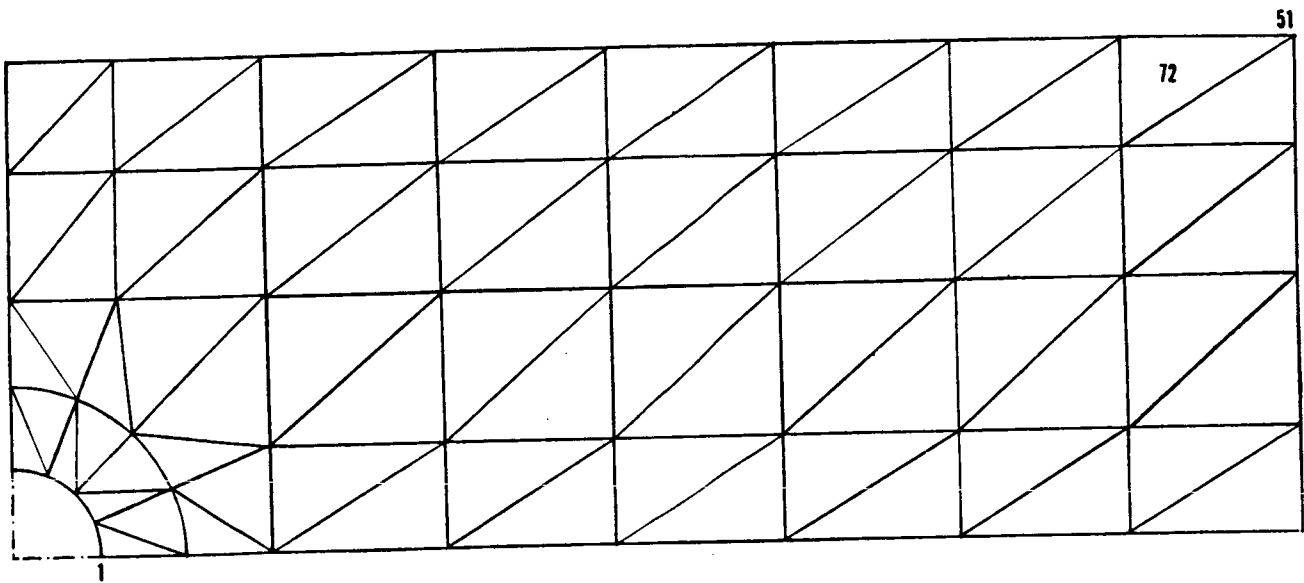


Figure 11. Discretization with 72 triangular elements

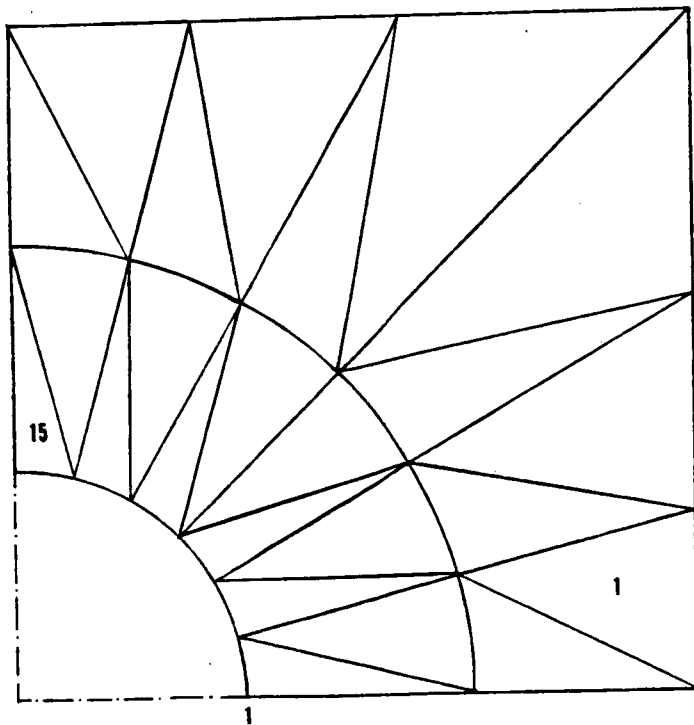
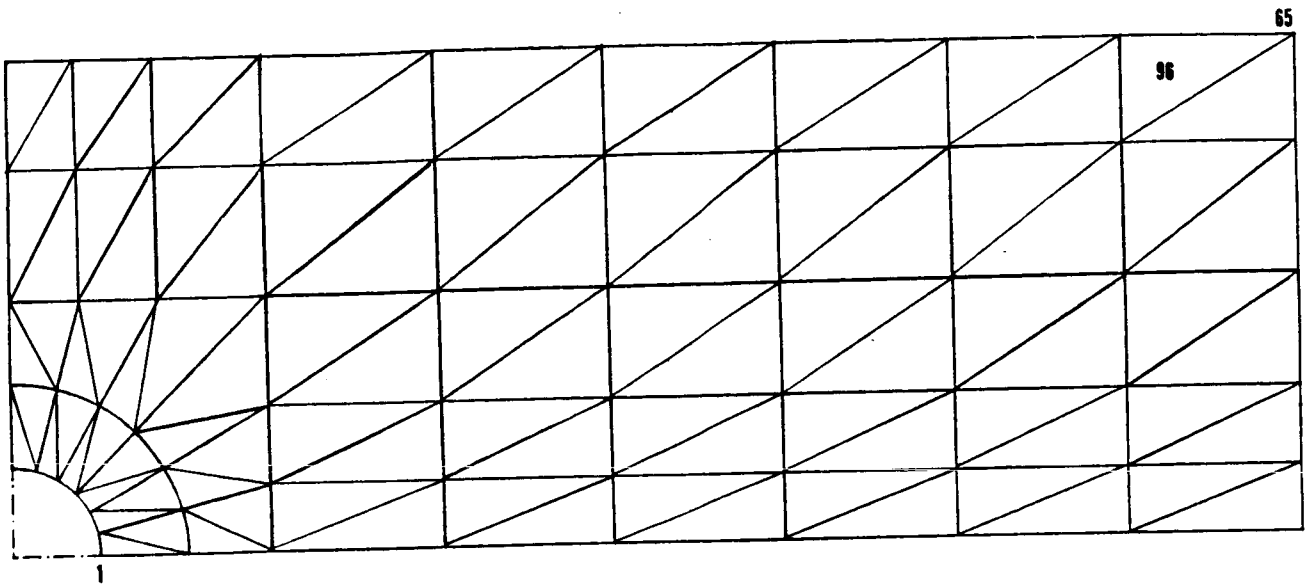


Figure 12. Discretization with 96 triangular elements

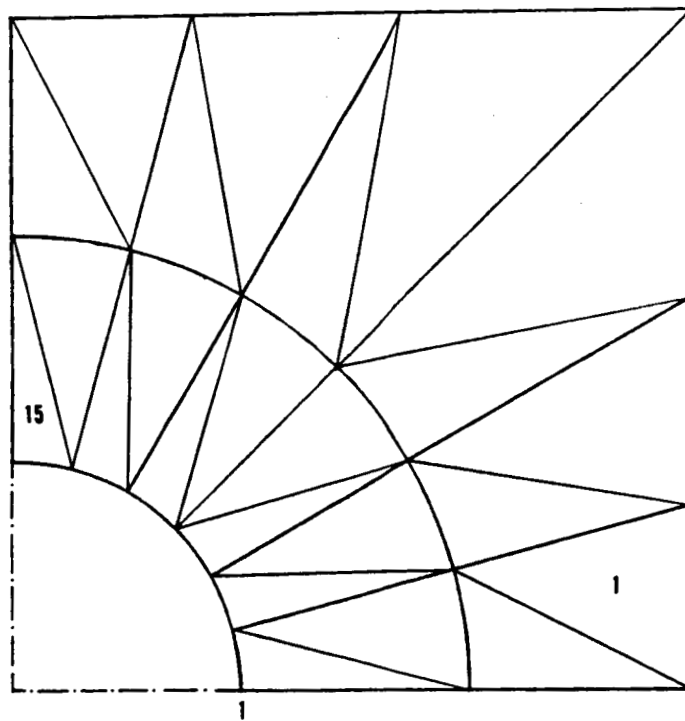
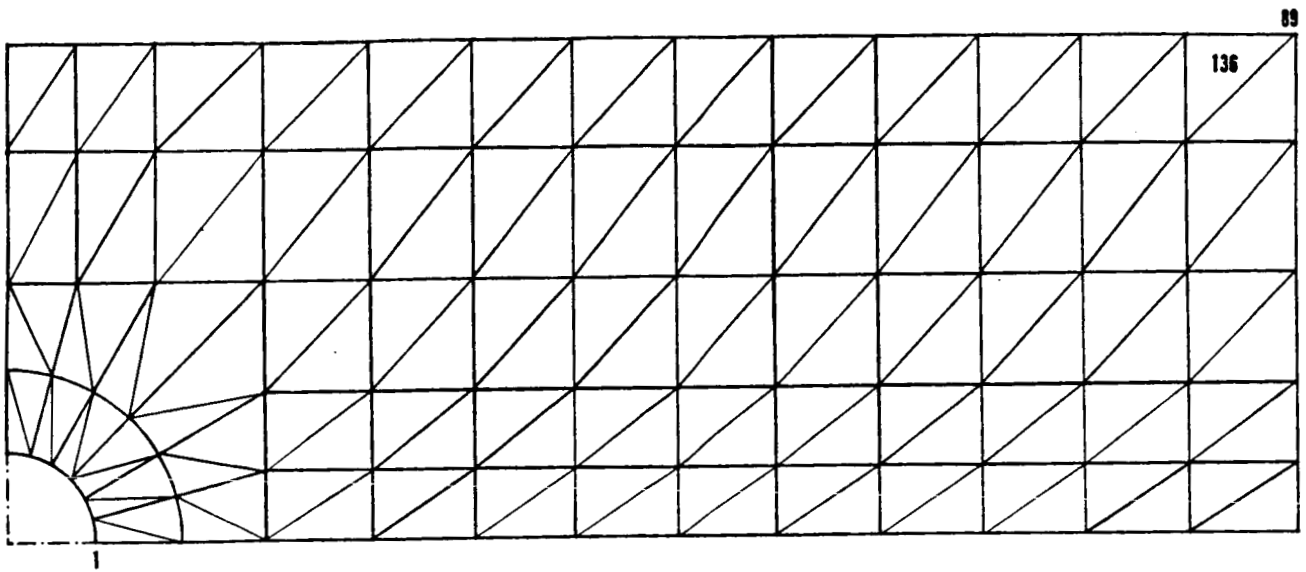


Figure 13. Discretization with 136 triangular elements

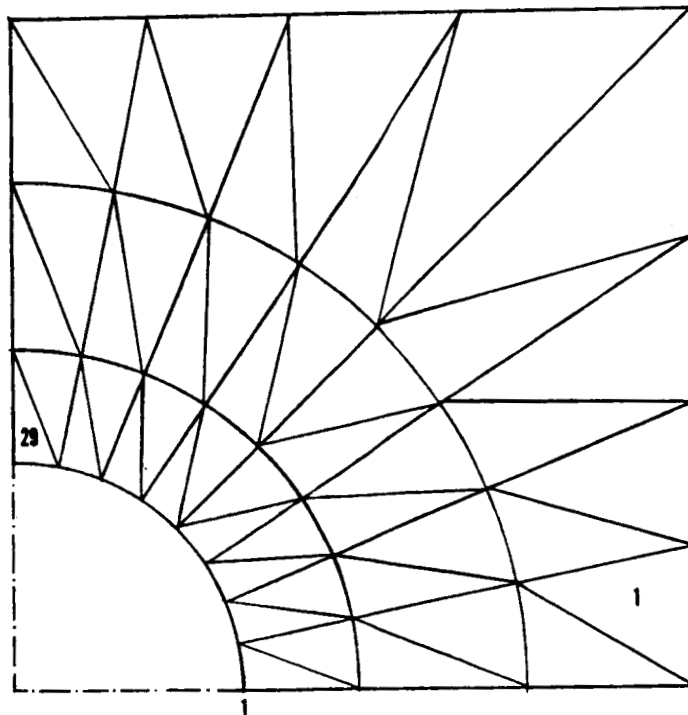
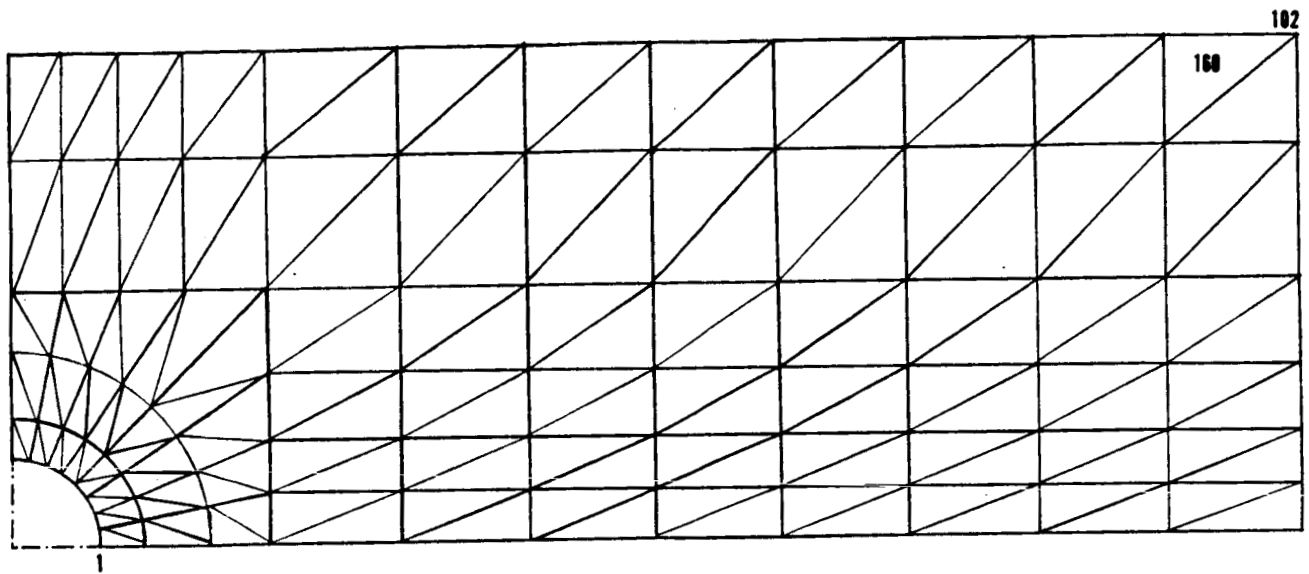


Figure 14. Discretization with 160 triangular elements

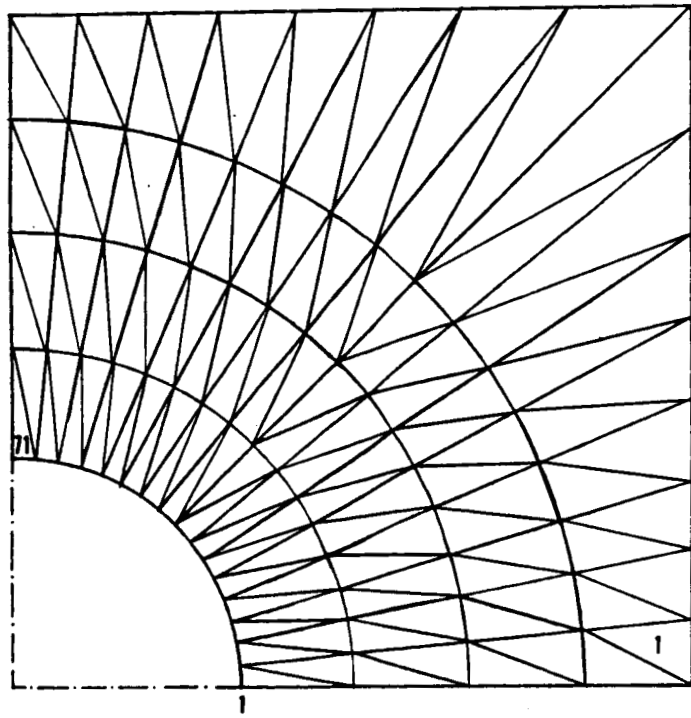
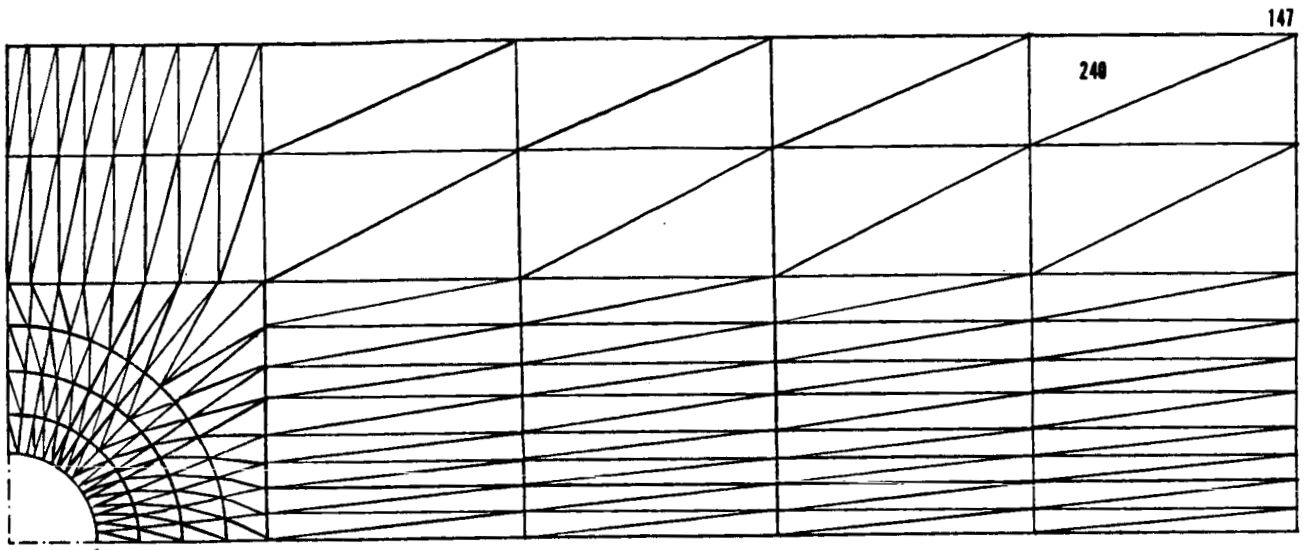


Figure 15. Discretization with 240 triangular elements

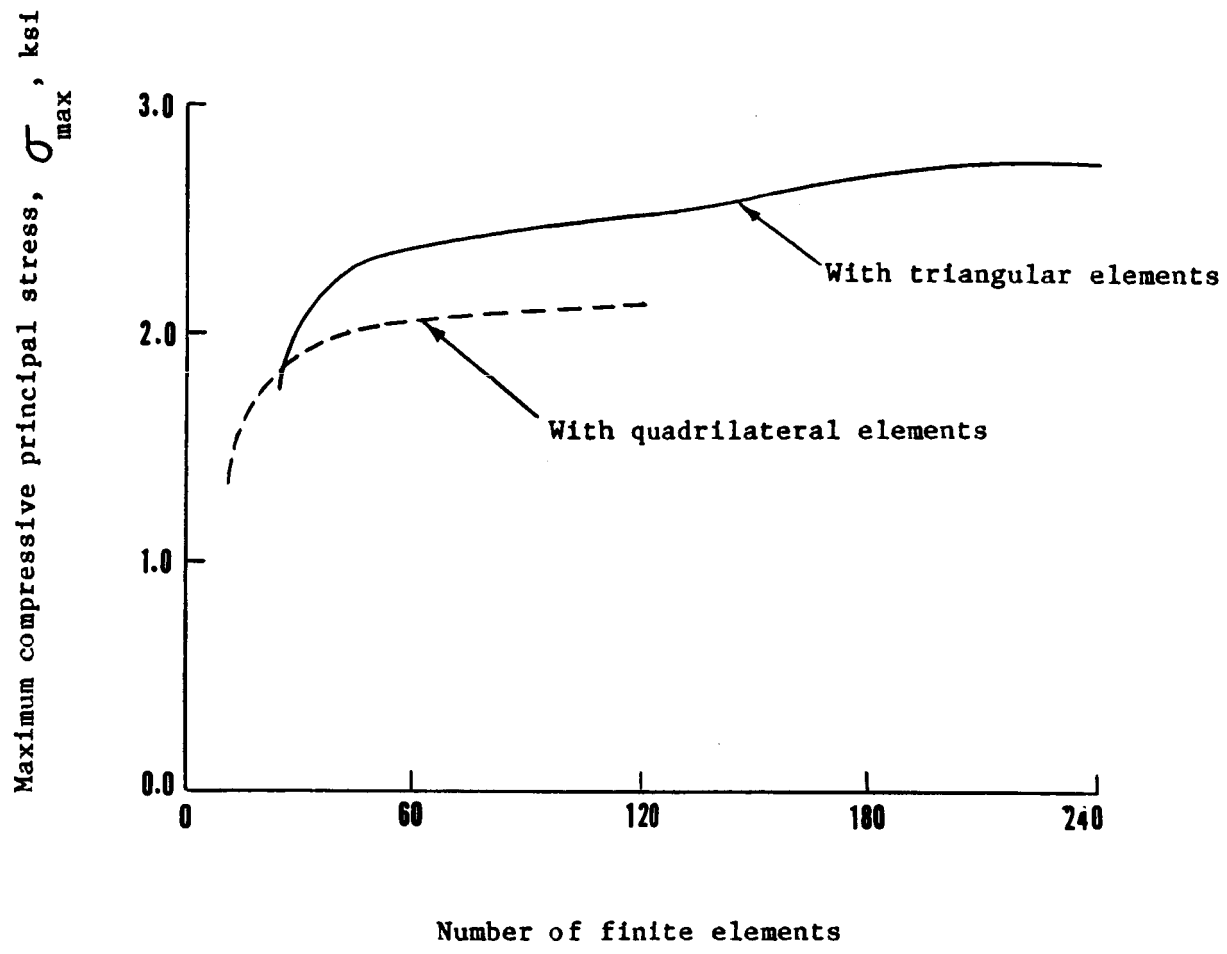


Figure 16. Maximum principal stress versus number of elements for isotropic panel

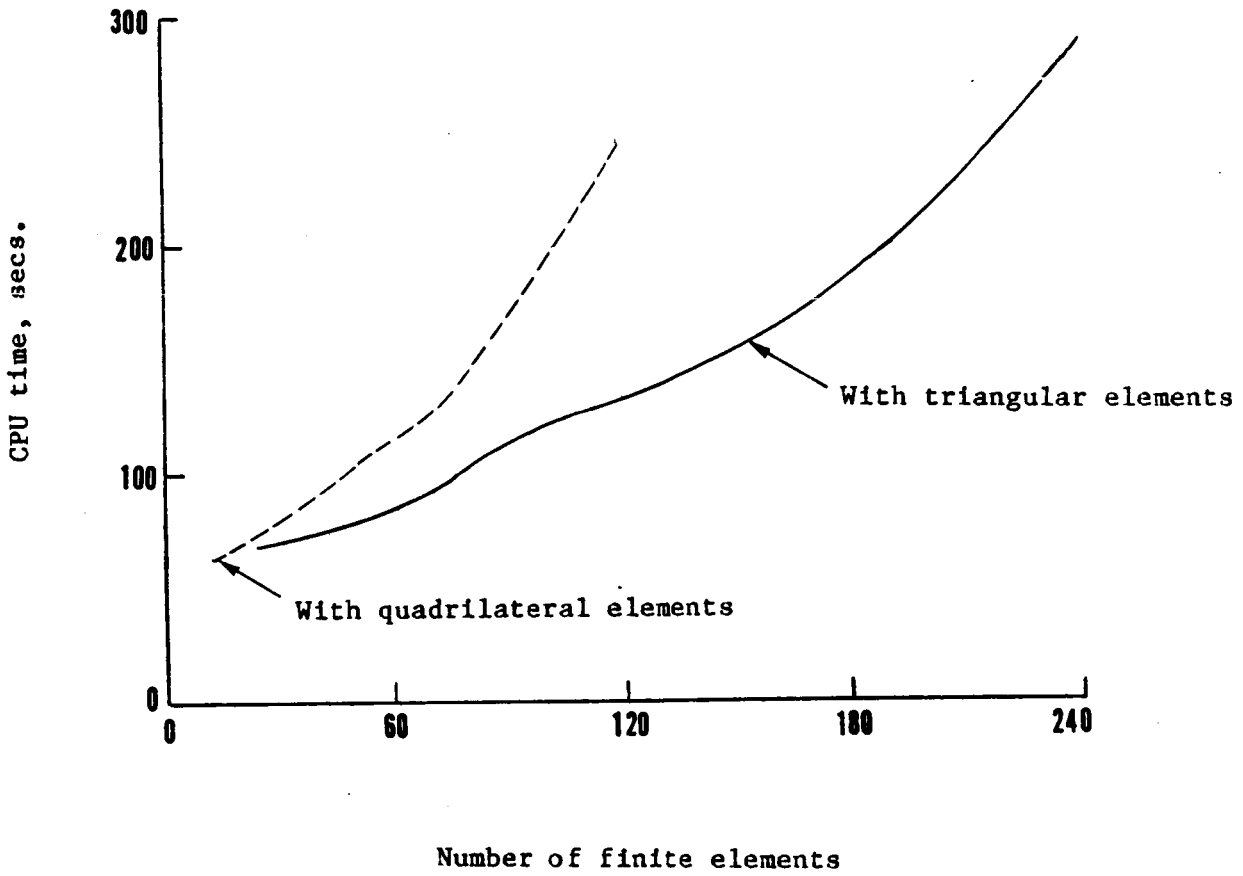


Figure 17. Computational time versus number of elements for isotropic panel

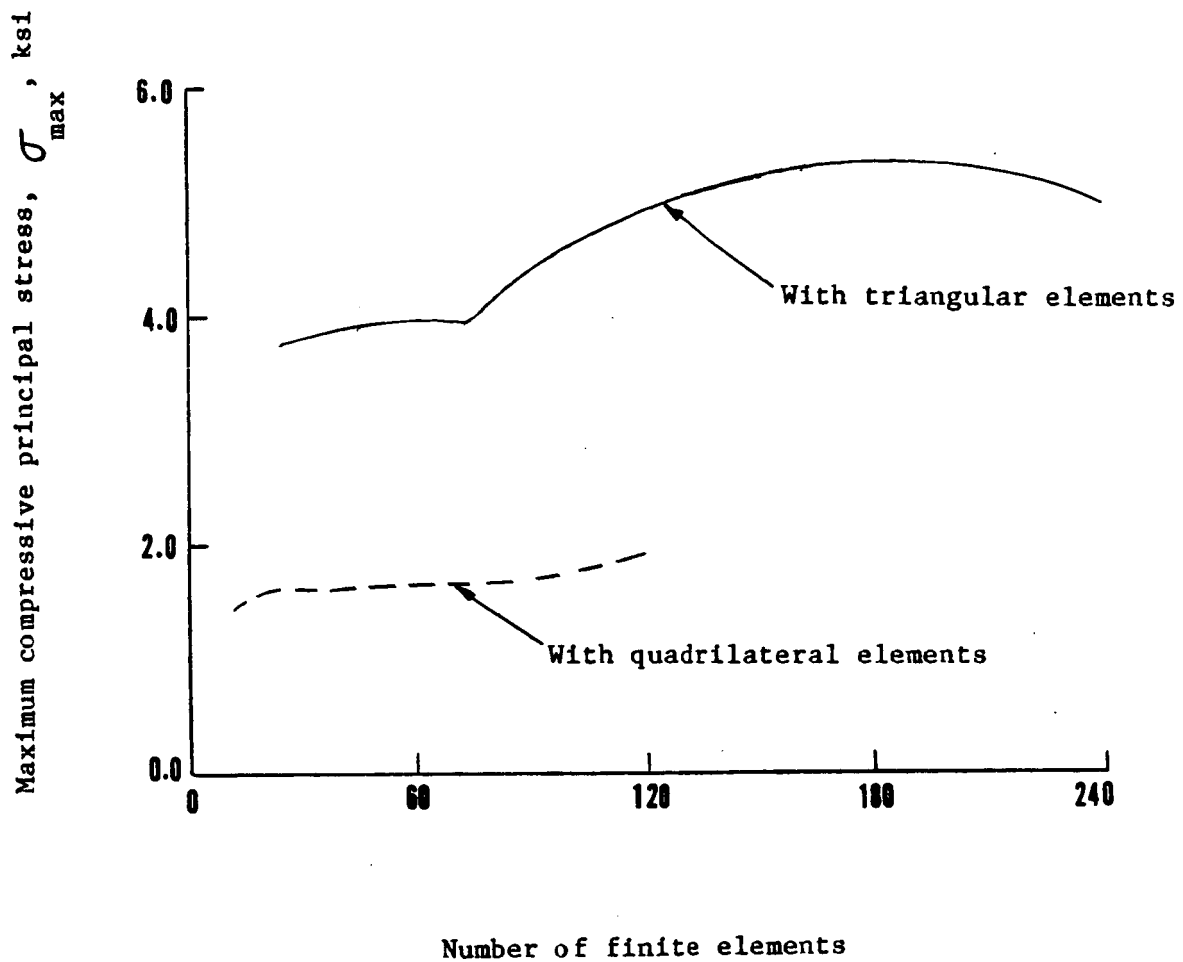


Figure 18. Maximum principal stress versus number of elements for orthotropic panel

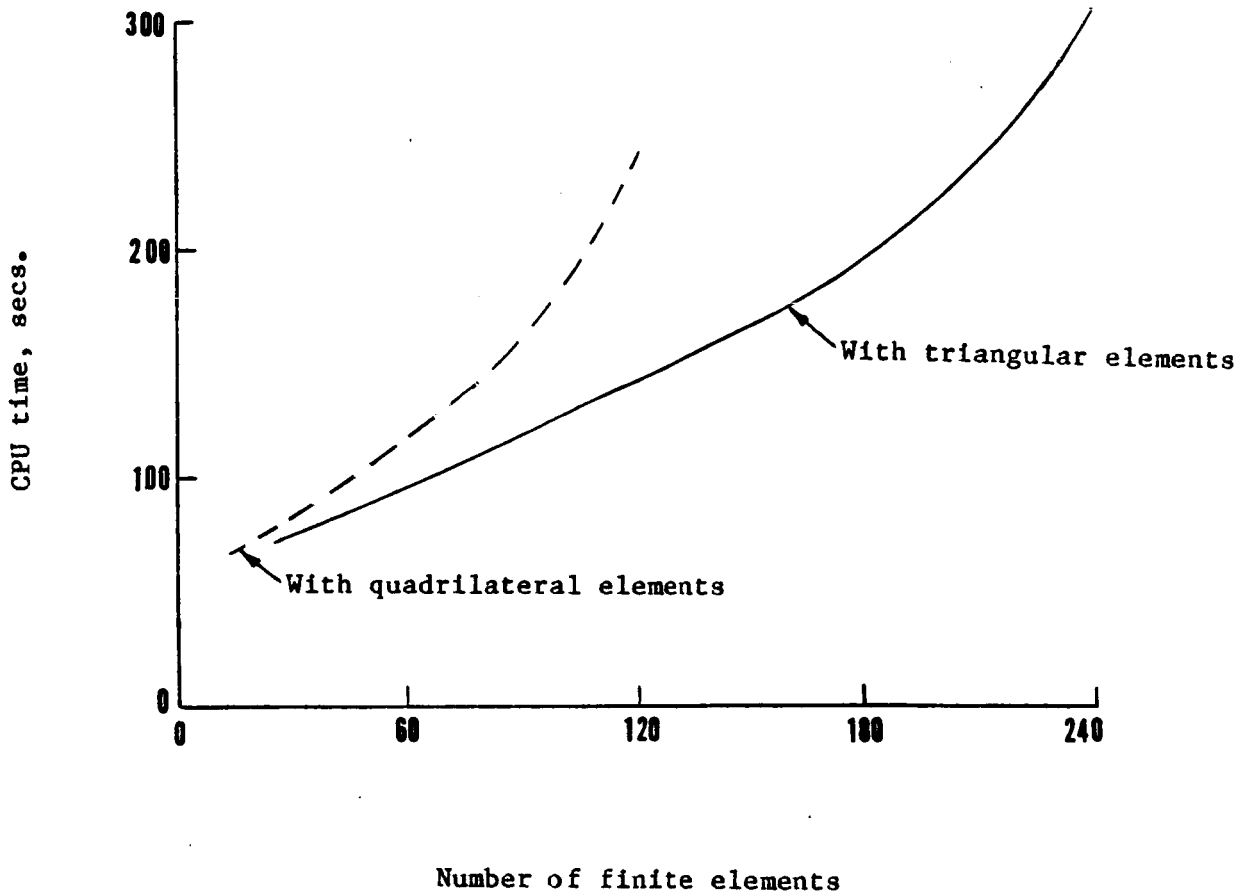


Figure 19. Computational time versus number of elements for orthotropic panel

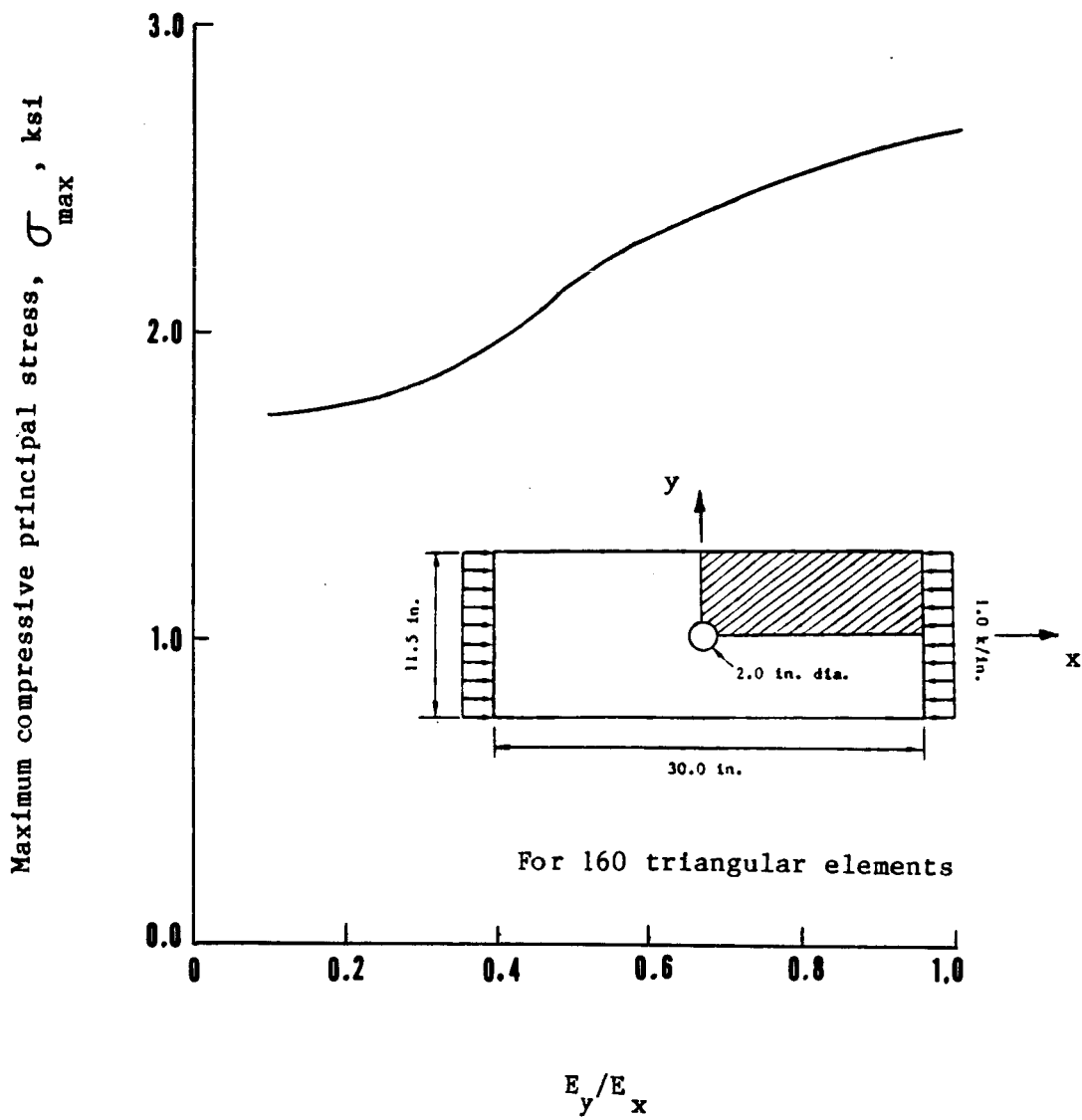


Figure 20. Maximum principal stress versus E_y/E_x ratio for orthotropic panel